Modification of graphene supported on SiO_2 substrate with swift heavy ions from atomistic simulation point

Shijun Zhao and Jianming Xue*

[1]State Key Laboratory of Nuclear Physics and Technology, School of Physics, Peking University, Beijing 100871, P. R. China

[2]Center for Applied Physics and Technology, Peking University, Beijing 100871, P. R. China

Abstract. The damage production induced by swift heavy ion (SHI) irradiations in graphene supported on a SiO_2 substrate is investigated using the molecular dynamics method. The thermal spike model is used to simulate the energy deposited into the lattice due to electron-phonon coupling. Our results indicate that the supported graphene could be damaged when the deposited energy per unit path length is higher than 6.5 keV/nm, which is higher than the threshold value for track formation in SiO_2. Therefore, the formation of ion tracks in the substrate is before the defect production in supported graphene and the rupture of graphene is initiated from the track core region. We further show that the defect production mechanism in supported graphene is due to the propagation of pressure waves resulting from the hot center of the ion track. Our results thus provide a mechanistic explanation for the reported modification of graphene with SHIs.

* Corresponding author. Tel: +86 (010)62758494. E-mail: jmxue@pku.edu.cn (J. Xue)

1. Introduction

Graphene is a truly one-atom-thick layer consisted of sp^2-bonded carbon atoms arranged in a honeycomb lattice.[1] Its intrinsic two-dimensional structure makes it attractive for many applications such as detecting single molecule gas,[2, 3] supercapacitors,[4, 5] solar cells,[6] field effect transistors,[7, 8] photonics and optoelectronics.[9] In view of its wide applications, significant amount of fundamental research is dedicated towards controllable modification of the properties of graphene in order to meet the needs of various application domains. In this context, ion irradiation as an effective tool has been used to introduce various defects in graphene[10-14] in order to engineer its properties.

Actually, energetic ions have been shown to be promising tools in doping graphene with foreign atoms and manipulating its structures both theoretically and experimentally.[14, 15] Until now, nearly all these applications utilize the effect of nuclear collisions between the incident ions and graphene, which is more efficient for low energetic ions due to their large nuclear stopping cross sections. For swift heavy ions (SHIs), the energy loss is dominated by ionizations and excitations of the target electrons, which subsequently transfer to the target lattice by electron-phonon coupling and result in a high local temperature.[16] Due to the excellent electric and thermal conductivities of graphene, it is usually thought that the electronic excitations have little influence on the graphene lattice. Recently it has been reported that graphene supported by dielectric materials could be torn apart under the irradiation of Xe^{23+} ions at 91 MeV.[17] In this case, the presence of the substrate seems to be a key factor in governing the behavior of supported graphene under irradiations. It was proposed that this phenomenon came from the formation of ion tracks in the substrate which subsequently led to the breakage of graphene since the effect of nuclear collisions can be neglected at this energy range. This provides a new way to manipulate graphene in a controlled manner, though the defect production mechanism is still unclear.

In experiments, SiO_2 is widely used as an insulating substrate for graphene to conduct physical property measurement and device fabrication.[18, 19] It has been demonstrated that the presence of SiO_2 substrate can have a vital effect on the final defect creation in supported graphene exposed to low energy particles as graphene can be damaged by backscattered particles and atoms sputtered from the substrate.[12-14, 20] For SHIs, the inelastic interactions prevail over nuclear collisions, which results in ion tracks in dielectric substrates such as SiO_2.[16]

However, the influence of ion track formation on the supported graphene remains a mystery, though limited available experimental observations indicate that extended damages along the ion track direction can be created with SHI irradiation at an oblique angle.[17, 21, 22] The track formation in materials such as silica has been successfully described by the thermal spike model,[16, 23] in which the energy of SHI is considered to dissipate from target electrons to lattice atoms through electron-phonon coupling at a short time scale. By assuming that the excited electron energy is absorbed by phonons within a radius defined by the initial electron energy distribution and the electron-phonon coupling strength, the classical molecular dynamics (MD) is capable to describe the damage mechanism of SHI to materials.[24, 25]

In this paper, we investigate the effect of SHI irradiation on graphene supported by a SiO_2 substrate with the MD method. The electronic energy loss to the target atoms is modeled by the thermal spike model. The influence of track formation in SiO_2 on the defect creation mechanism in graphene is discussed. Our results demonstrate that there is a threshold electronic energy loss for damage production in graphene, which is higher than that for track formation in SiO_2 substrate. The breakage of graphene is determined by the pressure waves induced by the thermal spike. We also simulate that how the glancing incident SHI could be used to cut and modify graphene along the ion path in a controlled way.

2. Computational details

Classical MD simulations were performed with the LAMMPS code.[26] The adaptive intermolecular reactive empirical bond-order (AIREBO) potential function[27] was employed to calculate the interaction between carbon atoms in graphene, which is derived from the second-generation Brenner potential (REBO).[28] This potential has been successfully used to simulate the irradiation effects in graphene before.[20, 29-31] The interactions of Si-Si, Si-O, O-O are described by Tersoff potentials[32] with parameters taken from Munetoh *et al*.[33] The forces between graphene and the substrate are assumed to be van der Waals (vdW) type modeled with the Lennard-Jones (LJ) potential $V_{ij}(r)=4\varepsilon_{ij}[(\sigma/r)^{12}-(\sigma/r)^{6}]$ where i=C, j=Si or O, and r is the interatomic distance. The parameterization of the numerical values ε_{ij} and σ is from Ong *et al*.[34] To model energetic collisions, the potential for Si and O was smoothly joined with the Ziegler-Biersack-Littmark (ZBL) potentials[35] at short interatomic separations, which include a

short-range repulsive force between all pairs of atoms to better describe the impact of atoms. More simulation details can be found in our previous paper.[20]

Graphene used in the simulation consisted of 12800 carbon atoms with the dimensions around 170 × 197 $Å^2$. The (0001) plane with O termination cleaved from SiO_2 bulk was used as substrate and the graphene sheet was then placed on it, as illustrated in Figure 1. The lattice mismatch between the graphene and SiO_2 slab is -0.14%. The thickness of the SiO_2 slab was chosen to be around 110 Å in *z* direction. The total atom number of the system is 300800.

The electronic excitations created by the swift ions are accounted for by giving certain kinetic energy to the atoms in a cylindrical region with a radius of 3 nm, as it has been done before for a variety of materials.[16, 24, 25, 36] The cylinder is located at the center of the *x*-*y* plane with the length spanning the whole simulation box in the z direction to simulate the normal incidence event. The electronic energy loss of SHI inducing the tracks is implemented by an instantaneous deposition of kinetic energy with a random direction to the atoms in a cylindrical region. After the full relaxation of the graphene-SiO_2 system, the kinetic energy is given as the initial conditions and the subsequent evolution is monitored.

In our simulations, all the atoms in the cylinder region are assigned the same kinetic energy but with random momentum directions. Two other initial kinetic energy distributions inside the track region including $1/r$ and Gaussian distribution are also tested, in which the energy is a constant value in the track core region with a radius of r_0 and then decays with r_0/r and $\exp[-(r^2 - r_o^2)/2]$. It is found that the defect structures formed by these different distributions are essentially the same, including the defect configurations in supported graphene. However, the threshold value for track formation and created defect size are dependent on the choice of r_0 and r in this case. In this work, we simply assign the same energy to the atoms inside the track region because in this theoretical work we do not know how to choose r in the above formula, which depends on the ion velocity.[37] With this simple model, the threshold energy for track formation and track radius is still reasonable compared with experimental data.[38]

Four runs initiated by different random number seeds for initial velocity are carried out. The simulated energy deposition per unit length (dE/dx) varies from 1 to 12 keV/nm, corresponding to an energy per atom from 0.45 to 5.44 eV. It should be noted that in reality, due to the limited electron-phonon coupling efficiency, not all the energy deposited in the electronic system can be converted to the kinetic energy of the atoms. Therefore, the corresponding experimental dE/dx is

expected to be larger than the values used in our simulations in order to achieve the same kinetic energy per atom.

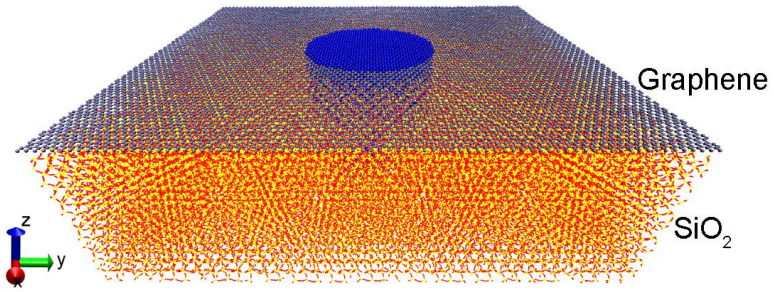

Figure 1 Illustration of the simulation setup. The blue region in the center stands for the thermal spike used to model the electronic excitations.

Periodic boundary conditions are imposed in the two lateral (*x*-*y*) directions. After the system is fully relaxed at room temperature of 300 K, the thermal spike is introduced into the central cylinder region. A Berendsen temperature control technique[39] is employed at the borders to prevent pressure waves induced by the thermal spike to return back to the impact region over periodic boundaries. During the collision phase, a microcanonical ensemble (NVE) in which the number of particles, the volume of the cell and the total energy of the system are kept constant is used and Newton's equations of motion are integrated with a variable time step depending on the atomic energy to ensure the maximum displacement of atoms is less than 0.05 Å. For each d*E*/d*x* value, the collisional phase is considered to be finished when the maximal kinetic energy of the atoms in the system is less than 0.85 eV. After the collisions are over, the MD simulations are carried out under the canonical ensemble and temperature is maintained at 300 K with the Nośe-Hoover algorithm.[40, 41] The system is allowed to relax for 100 ps with a time step of 1 fs and then the data collection is performed.

3. Results and discussion

After full relaxation of the graphene-SiO_2 substrate system, we begin to assign certain kinetic energy to all the atoms in the cylinder region including C, Si and O located in the center so as to model the thermal spike induced by swift heavy ion irradiation. This energy is dissipated to surrounding atoms through atomic collision cascades, which leads to defect formation in the system. Since we are interested in the response of graphene, we show in Figure 2 the defects

created in the graphene at final state as a function of the electronic energy loss as well as the corresponding energy per atom assigned at the beginning. The defect is defined as carbon atoms displaced more than 3 Å from their original lattice site. These results are averaged from four independent runs with different random seeds to create the initial velocity directions.

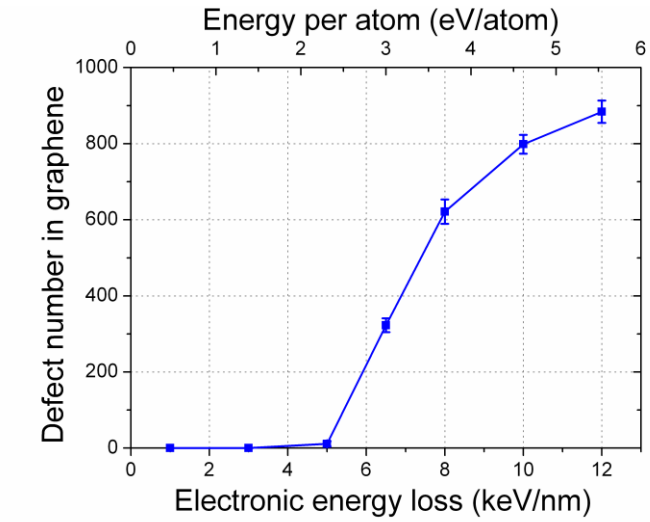

Figure 2. Dependence of defect number in the graphene on the electronic energy loss as well as corresponding energy per atom.

It can be seen from Figure 2 that there is a threshold value of d*E*/d*x* below which no damage could be found in the graphene. The value in our simulation is determined in the range from 5 to 6.5 keV/nm and the graphene is severely damaged at 6.5 keV/nm. Note that the non-zero defect number at 5 keV/nm is related to the defect statistic method that we used in this paper. At dE/d*x*=5 keV/nm, the calculated defect number is about 10, which is attributed to the formation of Stone-Wales defect and local distorted carbon rings. However, the whole graphene sheet is still intact. The damage in graphene becomes evident at dE/d*x*=6.5 keV/nm. Therefore, the threshold value for the rupture of graphene is determined at 6.5keV/nm. In our simulations, the track formation in SiO_2 is identified when d*E*/d*x* is 5 keV/nm with an amorphous region in the core, while it is not observed at 3 keV/nm. Therefore, the threshold value for track formation in SiO_2 should be in the range of 3-5 keV/nm, in line with previous results also with the thermal spike model which showed that a track is formed in quartz when the energy deposition is 4.5-5.1 keV/nm.[42] Since the main concern in this work is the damage of supported graphene induced by SHI due to the presence of SiO_2 substrate, our focus is on the role that the track plays in the

defect production process in graphene, but not the track formation process itself. For the latter, our systematic study about the MD simulations for the track formation process in α-quartz showed an excellent agreement with previous results.[38]

Thus, our results demonstrate that the threshold of dE/dx for defect production in supported graphene is greater than that for track formation in SiO_2. Therefore, the damage of supported graphene always goes together with track formation in the SiO_2 substrate assuming that the electronic excitation energy induced by SHI is converted to the atomic system instantaneously. The MD approach employed here cannot account for the electronic excitations directly. It can only be used to describe the evolution of the system after the energy has been transferred to the lattice atoms. In this case, we cannot exclude the possibility of direct damage in graphene induced by the electronic excitations before its energy is converted to atoms.

The larger threshold for the rupture of graphene can be understood in terms of bond strengths. Due to the good mechanical property of graphene,[43] more energy is required to break the C-C bond than to remove the Si or O atoms from SiO_2 surface. As a result, the threshold for the rupture of graphene is larger than that for track formation in SiO_2. It should be noted that this conclusion is irrespective of the initial energy distributions as mentioned in the previous section, since these initial energy distributions only affect the atomic motions in the rim of the spike region.

The defect created in graphene is seen to be a big nanopore located just at the thermal spike region. Figure 3 demonstrates the defect configurations observed for different dE/dx values. It indicates that the defect structure is created due to the loss of carbon atoms. As a result, a nanopore is formed in the graphene sheet with its center just positioned at the track core. When dE/dx is 6.5 keV/nm at which the graphene starts to rupture, those carbon atoms located at the center of the spike are all sputtered out while those at the edge are partially lost. Consequently, the defect configuration is composed of a relatively small central pore and surrounding mesh-like structure with lots of carbon chains. With increasing dE/dx values, the size of the nanopore is first increasing and then saturates as the track radius is set to 3 nm in our simulations. Due to the various possible hybridizations of carbon, it allows different numbers of nearest neighbors. For sp^2-hybridized carbon atoms, it can exhibit a variety of polygons besides common hexagons to form different structures. Because of this, vacancies in graphene tend to reconstruct by saturating dangling bonds and forming non-hexagonal rings via bond rotations.[44-46] These

non-hexagonal rings may either lead to curvature in the sheet or keep the sheet planar with some symmetric structures. In our simulations, the reconstruction of the atomic network of graphene near the vacancies is observed, which finally results in the defect configurations shown in Figure 3 after full relaxations. It can be seen that there are plenty of carbon pentagons, heptagons, and octagons as well as other non-hexagonal rings distributed at the edge of the pore, which are indeed created by the reconstruction of carbon atomic network. In addition, there are plenty of carbon chains observed in the rim of the created nanopore. These configurations are somewhat like those formed by the impact of energetic clusters.[29] It should be noted that the atomic carbon chains are energetic favorable and they are formed self-organized during the defect production. Two types of carbon chains are observed in the final state after long-time evolutions: one is the suspended free-hanging monatomic carbon chains with its end point attached to the edge of the nanopore, and the other is the carbon chain loops along the pore edges. At low dE/dx (Figure 3(a) and (b)), more carbon chain loops are found while suspended carbon chains appear mostly at high dE/dx values (Figure 3(c) and (d)). This is because the number of sputtered atoms from the thermal spike region increase with increasing dE/dx. As a result, more carbon atoms can be displaced far away from the graphene plane, which reduces the probability of atomic reconstructions. Consequently, more suspended carbon chains are formed at high dE/dx.

It has been pointed out that the presence of substrate would have a beneficial effect for the reconstruction of defective graphene by forming perfect hexagons or non-six member rings.[47, 48] In these cases, the substrate acts as a shield for displaced carbon atoms, which provides a reservoir of loose carbon atoms. These atoms can then be incorporated into the defect sites in the graphene lattice with a remarkable reknitting process. Here, the source of carbon atoms is the key to realize the self-healing capability of graphene either by knocked out atoms from neighboring edges or hydrocarbon contamination patches. However, this observation is absent in our simulations based on thermal spike model because the atoms in the spike region are almost all displaced. Only the atomic reconstructions at the edge of the nanopore are found, as revealed in suspended graphene before. [47]

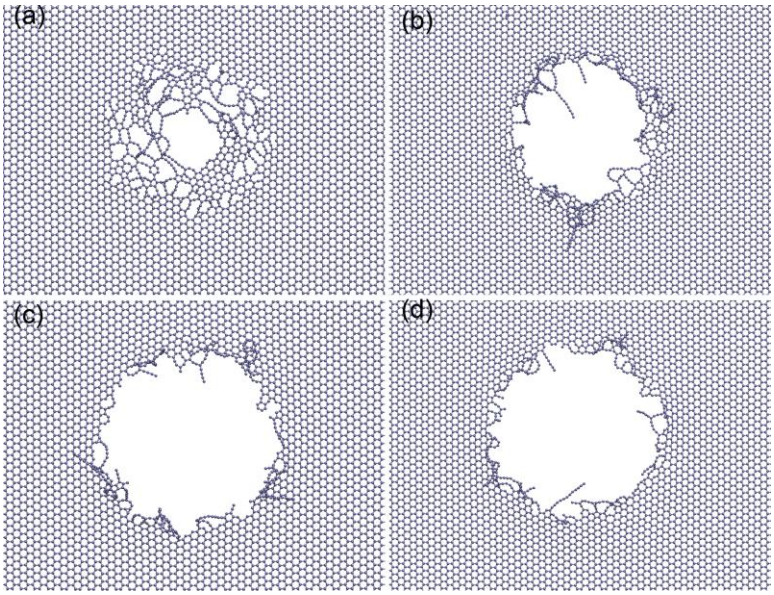

Figure 3. Defect configurations created in supported graphene for the following d*E*/d*x* values: (a) 6.5 keV/nm, (b) 8 keV/nm, (c) 10 keV/nm,(d) 12 keV/nm. Only graphene is shown for clarity.

In our simulations, the carbon atoms are found to be pulled out from the graphene plane due to the thermal spike. Since the nuclear stopping cross sections are negligible in this energy regime, the defects in graphene are not merely a direct result of the atomic collisions due to the kinetic energy deposited in the thermal spike region. It is demonstrated that the ejection of atoms is restricted to the thermal spike region, which is comparable to the case of localized excitations resulting from highly-charged ions.[49] In fact, previous experiment and MD simulations on particles emission from a cylindrically excited track in LiF and condensed rare gas targets revealed that ejected particles mostly originated from the first few monolayers in the track.[50-52] This behavior was interpreted in terms of emission due to a pressure-driven jet or a pressure pulse built up inside the track core, which led to a rapid expansion of particles in the track both laterally and upward and finally gives rise to the sputtering of particles.[53, 54] In view of these conclusions, it can be inferred that the stress initiated from the track region should play an important role in the damage process of supported graphene.

In order to further clarify why the graphene is damaged at the threshold d*E*/d*x* (6.5 keV/nm) although the kinetic energy per atom is only 2.95 eV/atom, we have analyzed the time evolution of kinetic energy and atomic stress in the *z* direction (σ_{zz}) of the graphene-SiO_2 system. Here we

show in Figure 4 three configurations when the breakage of graphene is initiated. It is demonstrated in Figure 4 that the maximal atomic kinetic energy (ke_{max}) of the graphene-SiO_2 system at the breaking point is 11.09 eV (Figure 4(c)). A distinct observation is that the breakage of the graphene is in the form of small clusters but not single atoms, which suggests that the rupture of graphene is the result of collective motion of all the atoms in the track region.

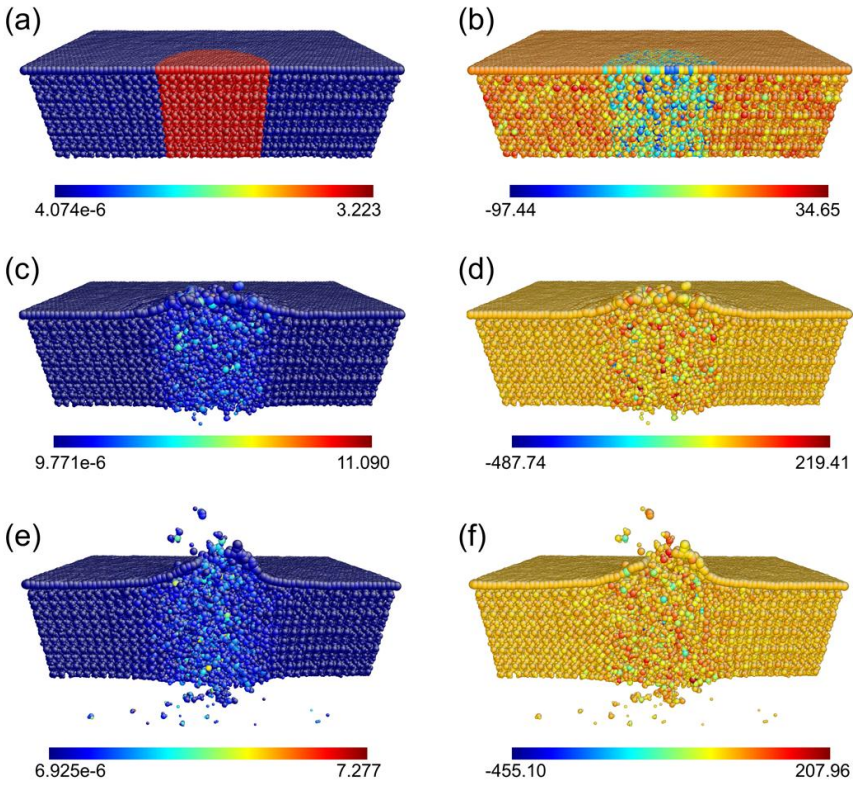

Figure 4. The temporal evolution of the kinetic energies (in eV, (a), (c) and (e) in left column) and atomic stresses in *z* direction (in GPa, (b), (d) and (f) in right column) of the graphene-SiO_2 system when the electronic energy loss is 6.5 keV/nm. The simulation time is 0 ps, 0.54 ps and 2.96 ps from the top row to the third row.

Further insight into the breakage mechanism of graphene can be gained from the distribution of per-atom stress in *z* direction as provided in Figure 4. It is indicated in Figure 4 (d) that the maximal σ_{zz} (σ_{zz}_max) in the system can achieve -487.74 GPa. Here, the negative stresses mean tensile forces imposed on the atoms. It is shown that the high stress is mainly localized in the track core region. In order to distinguish the effects of kinetic energy transfer and atomic stress distribution on the rupture process of graphene, the evolution of *ke*_max and $|\sigma_{zz}|\_max$ of all the

carbon atoms in graphene is provided in Figure 5(a) and 5(b), respectively. It is demonstrated that the *ke*_max of all the carbon atoms is always below 10 eV in the damage process, while $|\sigma_{zz}|$_max is as high as 280 GPa around 1 ps after the introduction of the thermal spike. In our simulations, the breakage of graphene is observed at 0.33 ps as shown in the Figure 6(a). There are already several cracks in the track region, which subsequently tears the graphene apart. At this stage, the $|\sigma_{zz}|$_max is seen to be fluctuating around 180 GPa. According to experimental results, the intrinsic stress of graphene is 130±10 GPa.[43] Consequently, we conclude that the damage in graphene results from the stress accumulation in the track region. The σ_{zz}_max of carbon atoms is even higher after the rupture is initiated. At 0.33 ps, several cracks have been developed, which lead to the rupture of carbon bonds and emission of carbon atoms subsequently at 0.50 ps as shown in Figure 4(c) and 4(d). The higher per-atom stress later corresponds to the ejection of carbon atoms. After that, a small pore is formed in the graphene and the per-atom stress is lowered.

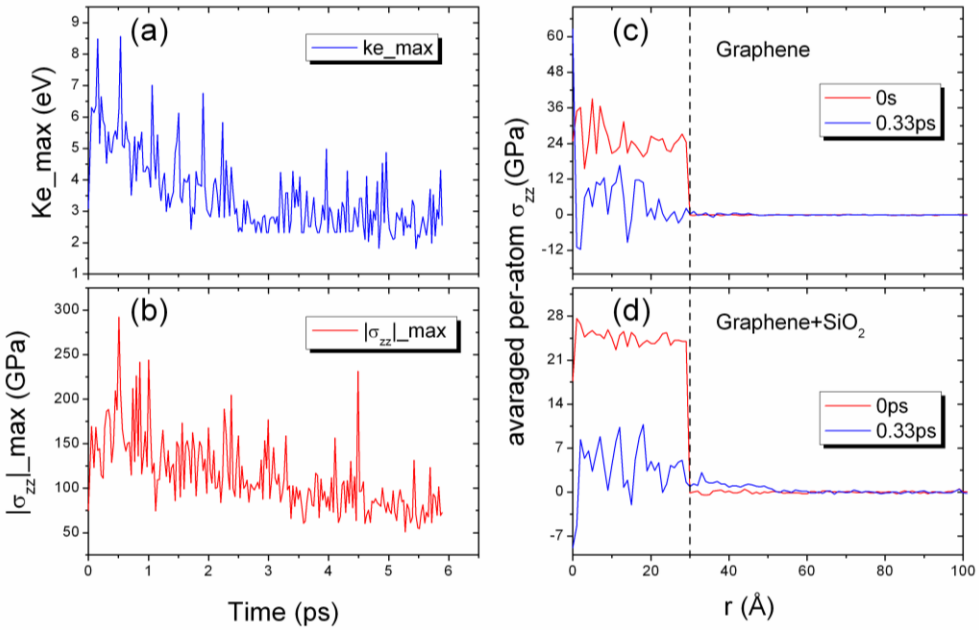

Figure 5. The temporal evolution of the (a) maximal kinetic energy and (b) maximal atomic stress in *z* direction extracted from all the carbon atoms of the graphene when d*E*/d*x* is 6.5 keV/nm. The average distributions of the per-atom σ_{zz} of (c) supported graphene and (d) graphene-SiO_2 system along the radial distance from the center of the track are also plotted. Two different evolution time are provided: one is initial state (0 ps) and the other is just when the graphene starts to break (0.33 ps). The track

radius is located at 30 Å, as indicated by the dashed line.

It has been demonstrated that the track structure in SiO_2 is comprised of a low density core surrounded by a high density shell.[16] During the initial stage of the thermal spike, the pressure wave gives rise to a flow of constituent atoms from the center of the track to the surrounding regions. In this case, due to the presence of the surface, more atoms can be pushed out by the pressure wave as there are no obstacles in this direction, as can be identified in Figure 4(d) and 4(f). As a result, those carbon atoms of graphene in the spike area are knocked out from their equilibrium position along with some Si and O atoms from the substrate. Finally, an amorphous cylinder at the center of the track is formed with low density core, in line with experimental measurements.[16] It should be noted that only atoms in the thermal spike region are ejected due to the presence of the pressure wave since the defect configuration produced in graphene is a nanopore with its size close to the spike region. This observation is in agreement with previous arguments that the SHI irradiations led to the ejection of atoms in the substrate which can cause the doping of graphene.[22] In our simulations, the doping of graphene is also observed at the edge of the track region but with an unstable structure because of the weak LJ interactions used between graphene and Si and O atoms.

Upon closer inspection, we find that those atoms which escaped from the upper surface are in the form of clusters instead of single atoms, as can be seen in Figure 4(e) and 4(f). This observation further supports our conclusion that the breakage of graphene results from the evolution of pressure waves initiated at the center of ion track. The average per-atom σ_{zz} in the graphene and graphene-SiO_2 system as a function of radial distance r from the center of the track is displayed in Figure 5(c) and 5(d), respectively. The distribution at initial state (0 ps) and the breaking point of graphene (0.33 ps) is provided, respectively. It is seen that σ_{zz} in the center is uniform due to the uniform kinetic energy distribution at the initial state. Besides, σ_{zz} in the track region is always higher than in other areas. As a consequence, a pressure wave emanates outwards. When the graphene starts to break, a much higher σ_{zz} in the track center (r=0 Å) is identified (Figure 5(c)). This observation accounts for the defect structure shown in Figure 3(a), which displays a pore in the center along with surrounding carbon chain loops. Furthermore, the atoms in the track region are displaced at the same time. As a result, these atoms escape from the system in the form of clusters.

The pressure wave can be directly identified from the atomic configurations. The atomic configurations at 0.33 ps when the graphene begins to break and 5.90 ps when several carbon atoms starts to escape from graphene are shown in the Figure 6. It can be seen that a pressure wave developes from the track center region and spread out, which gives rise to the ejection of atoms.

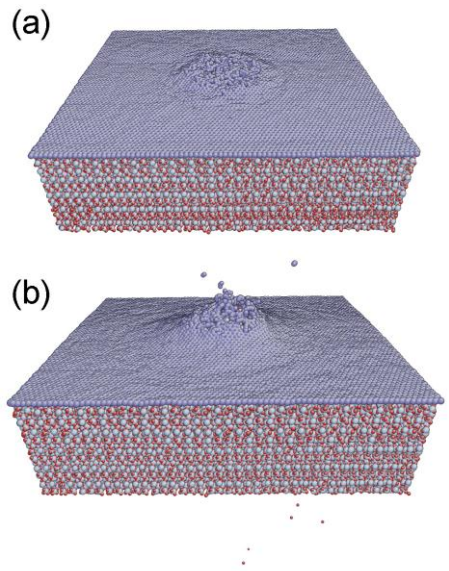

Figure 6. The atomic configurations of graphene-SiO_2 system (a) when the graphene begins to break and (b) when a nanopore starts to take shape. The pressure wave initiated from the track core region can be identified.

In this work, the simulations are performed only for the graphene-SiO_2 system. The simulations for suspended graphene are not included because how to model the electronic stopping in graphene is still unclear. Due to the excellent thermal and electrical conductivity of graphene, graphene should be difficult to be damaged by electronic excitations and ionizations since these effects can be dissipated very quickly, which means that the swift heavy ions can pass through it without creating substantial damage.[30, 31] For this reason, we did not perform simulations on suspended graphene with the thermal spike model as we realized that this model is not appropriate in this case. Specifically, the energy deposition in suspended monolayer graphene treated with a two-temperature model may not be valid since the excitations will be rapidly diffused away from each other and spread out the deposited region. As a matter of fact, the suspended graphene should be very stable under ion irradiations, so that it is suggested that

graphene can be used as the vacuum window for separating a high-vacuum ion beam system from targets kept at ambient conditions.[31]

In our simulations, all the atoms including C, Si and O atoms in the thermal spike region are given the same kinetic energy with random velocity directions. Although the direct energy transfer between SHI and graphene is unlikely to occur as discussed before, the graphene supported by SiO_2 substrate can still be heated by the secondary electron emission from the SiO_2 due to the deposition of a huge amount of energy to electrons in a highly localized region along the ion path. While most of these energy is used for track formation, the rest of the energy is dissipated by secondary electrons which leave the track region and eject into the volume surrounding the ion tracks.[55] In the presence of a surface, these electrons can escape from the material. Actually, a lot of work has been done to investigate the properties of secondary electrons emitted from the target including their numbers, their energy and angular distributions.[56, 57] In this case, the supported graphene which is located on the upper surface of SiO_2 is directly exposed to these secondary electrons, which results in a local heating effect in supported graphene. In view of this effect, we have assigned carbon atoms in the track region the same kinetic energy as Si and O atoms. Although it is unlikely that the radius of the thermal spike in supported graphene is the same as in SiO_2, our simulation provides a reasonable description of the damage process in graphene.

The damage production process in supported graphene is found to be critically related to the track formation in SiO_2 substrate. The track formation in SiO_2 resulting in sputtered Si and O atoms, which can collide with carbon atoms in graphene and finally lead to the defect formation in the graphene lattice. The track formation in SiO_2 is a prerequisite for the creation of an amorphous region which gives rise to the outwardly moving Si or O atoms. Therefore, the role of the substrate played in this process is that the track formation provides sputtered atoms which collide with graphene and finally lead to the defect formation in supported graphene, as argued in a previous paper.[21] This is different from the case of graphite irradiated with SHI, which showed a discontinuous sequence of damage segments instead of a homogeneous cylinder.[58] In our case, the sputtered Si or O atoms provide a possibility to dope graphene as a previous paper deduced.[22]

In our method, the graphene alone can still be damaged if we assign energies to carbon atoms in the center region. To further make clear whether the breakage of graphene is ascribed to the

presence of substrate or just a result of the kinetic energies we assigned, we have performed additional simulations in which only the atoms in substrate are given energies while assigning no extra kinetic energies to carbon atoms. The results show that some vacancy defects are created in graphene at dE/dx=6.5 keV/nm. On the contrary, if energies are only given to a suspended graphene, it starts to rupture when dE/d*x* is 8 keV/nm assuming that the thickness of suspended graphene is 3.4 Å. Thus our results presented in this paper highlight the role of SiO_2 substrate and give a lower limit of dE/d*x* for the damage of supported graphene in SiO_2 substrate.

Having discussed the damage mechanism of supported graphene under normal incidence of SHI, we now turn to the effect of oblique incidence. In this case, the cylinder was tilted at a large angle from the *z* axis to investigate the response of the supported graphene to the irradiation of SHI under oblique angles. All the atoms including surface atoms and those atoms inside this cylinder region are given the same energy of 5 eV. Here we show in Figure 7 the results obtained from three runs with different incident angles: 30˚, 10˚ and 3˚. The first column in Figure 7 demonstrates the distribution of initial kinetic energy in a slice through the center of the track. Due to the variation of projected range of ions, the thermal spike region is enlarged and d*E*/d*x* is determined to be 2.48, 4.86 and 7.74 keV/nm, corresponding to these three simulation setups.

We can see from Figure 7 that the carbon atoms initially located at the thermal spike region (indicated by red atoms) are almost gone at the end after full relaxation. These atoms depart from the graphene-SiO_2 system and move along the +*z* direction as time evolves. The pressure wave induced by the spike pushes the carbon atoms in supported graphene away and gives rise to a line of extended defects. This observation is in excellent agreement with the experimental findings that glancing incidence of SHI could unzip the graphene along the ion track direction.[17] Our simulation results indicate that the breakage of graphene results from the pressure wave originating from the center of the track. When the pressure wave reaches the surface, the atoms in the vicinity are expelled from the system. As graphene is laid on the surface of SiO_2, the carbon atoms in the spike region could be displaced along with the expansion of SiO_2 around the hot track core and just escape. Here, the presence of surface is the key to understanding the damage of graphene as it is more vulnerable to pressure waves caused by the thermal spike core compared to the bulk material.

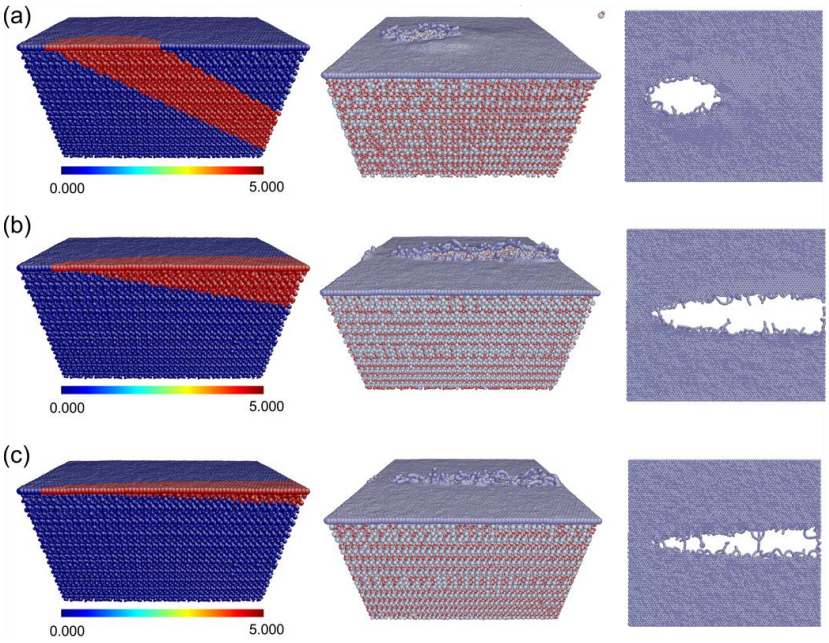

Figure 7. Simulation setup of SHI irradiations in three glancing angles and the final defect configurations resulted: (a) 30˚, (b) 10˚, (c) 3˚. The first column shows the distribution of initial kinetic energy (in eV) in a slice through the center of ion tracks. The second column is the side view of the final defect configurations and the third column corresponds to top view of the defects observed in supported graphene.

4. Summary

We have investigated the effect of SHI irradiation on supported graphene laid on SiO_2 substrate by means of classical MD simulations. The electronic energy loss of SHI and subsequent electron-phonon coupling is implemented by an instantaneous deposition of kinetic energy in a random direction to the atoms in a cylindrical region with a radius of 3 nm. Our results indicate that the formation of ion track in SiO_2 is always prior to the damage of supported graphene assuming that the electronic excitation energy induced by SHI is converted to the atomic system instantaneously. We further show that the defect production mechanism in graphene is due to the pressure wave resulting from the hot center of the ion track. Finally, we simulate how the SHI can be used to unzip graphene along the direction of ion tracks. Our results thus provides a possible mechanism for the modification of supported graphene due to SHI irradiations.

Acknowledgments

This work is financially supported by by the Ministry of Science and Technology of China (Grant No. 2010CB832904) and by NSAF (Grant No. U1230111), NSFC (Grant No. 91226202).

References

[1] Novoselov KS, Geim AK, Morozov SV, Jiang D, Zhang Y, Dubonos SV, et al., Electric field effect in atomically thin carbon films. Science 2004; 306(5696):666-9.

[2] Sint K, Wang B, Kr á l P, Selective ion passage through functionalized graphene nanopores. J. Am. Chem. Soc. 2008; 130(49):16448-9.

[3] Humplik T, Lee J, O'Hern SC, Fellman BA, Baig MA, Hassan SF, et al., Nanostructured materials for water desalination. Nanotechnology 2011; 22(292001.

[4] Stoller MD, Park S, Zhu Y, An J, Ruoff RS, Graphene-based ultracapacitors. Nano Lett. 2008; 8(10):3498-502.

[5] Yoo JJ, Balakrishnan K, Huang J, Meunier V, Sumpter BG, Srivastava A, et al., Ultrathin planar graphene supercapacitors. Nano Lett. 2011; 11(4):1423-7.

[6] Wang X, Zhi L, Mullen K, Transparent, conductive graphene electrodes for dye-sensitized solar cells. Nano Lett. 2007; 8(1):323-7.

[7] Meric I, Han MY, Young AF, Ozyilmaz B, Kim P, Shepard KL, Current saturation in zero-bandgap, top-gated graphene field-effect transistors. Nat. Nanotechnol. 2008; 3(11):654-9.

[8] Xia F, Farmer DB, Lin Y-m, Avouris P, Graphene field-effect transistors with high on/off current ratio and large transport band gap at room temperature. Nano Lett. 2010; 10(2):715-8.

[9] Bonaccorso F, Sun Z, Hasan T, Ferrari A, Graphene photonics and optoelectronics. Nat. Photonics 2010; 4(9):611-22.

[10] Tapaszt ó L, Dobrik G, Nemes-Incze P, Vertesy G, Lambin P, Bir ó LP, Tuning the electronic structure of graphene by ion irradiation. Phys. Rev. B 2008; 78(23):233407.

[11] Chen J-H, Cullen WG, Jang C, Fuhrer MS, Williams ED, Defect scattering in graphene. Phys. Rev. Lett. 2009; 102(23):236805.

[12] Stolyarova E, Stolyarov D, Bolotin K, Ryu S, Liu L, Rim KT, et al., Observation of graphene bubbles and effective mass transport under graphene films. Nano Lett. 2008; 9(1):332-7.

[13] Compagnini G, Giannazzo F, Sonde S, Raineri V, Rimini E, Ion irradiation and defect formation in

single layer graphene. Carbon 2009; 47(14):3201-7.
[14] Mathew S, Chan TK, Zhan D, Gopinadhan K, Barman AR, Breese MBH, et al., The effect of layer number and substrate on the stability of graphene under mev proton beam irradiation. Carbon 2011; 49(5):1720-6.
[15] Lehtinen O, Kotakoski J, Krasheninnikov AV, Keinonen J, Cutting and controlled modification of graphene with ion beams. Nanotechnology 2011; 22(17):175306.
[16] Kluth P, Schnohr CS, Pakarinen OH, Djurabekova F, Sprouster DJ, Giulian R, et al., Fine structure in swift heavy ion tracks in amorphous sio_2. Phys. Rev. Lett. 2008; 101(17):175503.
[17] Akcöltekin S, Bukowska H, Peters T, Osmani O, Monnet I, Alzaher I, et al., Unzipping and folding of graphene by swift heavy ions. Appl. Phys. Lett. 2011; 98(10):103103.
[18] Ishigami M, Chen JH, Cullen WG, Fuhrer MS, Williams ED, Atomic structure of graphene on sio_2. Nano Lett. 2007; 7(6):1643-8.
[19] Nguyen TC, Otani M, Okada S, Semiconducting electronic property of graphene adsorbed on (0001) surfaces of sio_2. Phys. Rev. Lett. 2011; 106(10):106801.
[20] Zhao S, Xue J, Wang Y, Yan S, Effect of sio_2 substrate on the irradiation-assisted manipulation of supported graphene: A molecular dynamics study. Nanotechnology 2012; 23(28):285703.
[21] Ochedowski O, Bussmann BK, d'Etat BB, Lebius H, Schleberger M, Manipulation of the graphene surface potential by ion irradiation. Appl. Phys. Lett. 2013; 102(15):153103-4.
[22] Ochedowski O, Marinov K, Wilbs G, Keller G, Scheuschner N, Severin D, et al., Radiation hardness of graphene and mos_2 field effect devices against swift heavy ion irradiation. J. Appl. Phys. 2013; 113(21):214306-7.
[23] Bonfiglioli G, Ferro A, Mojoni A, Electron microscope investigation on the nature of tracks of fission products in mica. J. Appl. Phys. 1961; 32(12):2499-503.
[24] Zhang J, Lang M, Ewing RC, Devanathan R, Weber WJ, Toulemonde M, Nanoscale phase transitions under extreme conditions within an ion track. J. Mater. Res. 2010; 25(07):1344-51.
[25] Caron M, Rothard H, Toulemonde M, Gervais B, Beuve M, Theoretical and experimental study of electronic temperatures in heavy ion tracks from auger electron spectra and thermal spike calculations. Nucl. Instrum. Methods Phys. Res. B 2006; 245(1):36-40.
[26] Plimpton S, Fast parallel algorithms for short-range molecular dynamics. J. Comput. Phys. 1995; 117(1):1-19.
[27] Stuart SJ, Tutein AB, Harrison JA, A reactive potential for hydrocarbons with intermolecular interactions. J. Chem. Phys. 2000; 112(6472.
[28] Brenner DW, Shenderova OA, Harrison JA, Stuart SJ, Ni B, Sinnott SB, A second-generation reactive

empirical bond order (rebo) potential energy expression for hydrocarbons. J. Phys.: Condens. Matter 2002; 14(783.

[29] Zhao SJ, Xue JM, Liang L, Wang YG, Yan S, Drilling nanopores in graphene with clusters: A molecular dynamics study. J. Phys. Chem. C 2012; 116(21):11776-82.

[30] Lehtinen O, Kotakoski J, Krasheninnikov AV, Tolvanen A, Nordlund K, Keinonen J, Effects of ion bombardment on a two-dimensional target: Atomistic simulations of graphene irradiation. Phys. Rev. B 2010; 81(15):153401.

[31] Ahlgren EH, Kotakoski J, Lehtinen O, Krasheninnikov AV, Ion irradiation tolerance of graphene as studied by atomistic simulations. Appl. Phys. Lett. 2012; 100(23):233108-4.

[32] Tersoff J, Modeling solid-state chemistry: Interatomic potentials for multicomponent systems. Phys. Rev. B 1989; 39(8):5566-8.

[33] Munetoh S, Motooka T, Moriguchi K, Shintani A, Interatomic potential for si-o systems using tersoff parameterization. Comput. Mater. Sci. 2007; 39(2):334-9.

[34] Ong Z-Y, Pop E, Molecular dynamics simulation of thermal boundary conductance between carbon nanotubes and sio_2. Phys. Rev. B 2010; 81(15):155408.

[35] Ziegler JF, Biersack JP, Littmark U, *The stopping and range of ions in matter*,Pergamon, New York (1985).

[36] Moreira PAFP, Devanathan R, Weber WJ, Atomistic simulation of track formation by energetic recoils in zircon. J. Phys.: Condens. Matter 2010; 22(39):395008.

[37] Afra B, Rodriguez MD, Trautmann C, Pakarinen OH, Djurabekova F, Nordlund K, et al., Saxs investigations of the morphology of swift heavy ion tracks in α-quartz. J. Phys.: Condens. Matter 2013; 25(4):045006.

[38] Lan Chun E, Xue J-M, Wang Y-G, Zhang Y-W, Molecular dynamics simulation of latent track formation in α-quartz. Chinese Physics C 2013; 37(3):038201.

[39] Berendsen HJC, Postma JPM, Van Gunsteren WF, DiNola A, Haak JR, Molecular dynamics with coupling to an external bath. J. Chem. Phys. 1984; 81(3684.

[40] Nosé S, A molecular dynamics method for simulations in the canonical ensemble. Mol. Phys. 1984; 52(2):255-68.

[41] Hoover WG, Canonical dynamics: Equilibrium phase-space distributions. Phys. Rev. A 1985; 31(3):1695.

[42] Klaumünzer S, Ion tracks in quartz and vitreous silica. Nucl. Instrum. Methods Phys. Res. B 2004; 225(1–2):136-53.

[43] Lee C, Wei X, Kysar JW, Hone J, Measurement of the elastic properties and intrinsic strength of

monolayer graphene. Science 2008; 321(5887):385-8.
[44] Kotakoski J, Krasheninnikov AV, Kaiser U, Meyer JC, From point defects in graphene to two-dimensional amorphous carbon. Phys. Rev. Lett. 2011; 106(10):105505.
[45] Kalbac M, Lehtinen O, Krasheninnikov AV, Keinonen J, Ion-irradiation-induced defects in isotopically-labeled two layered graphene: Enhanced in-situ annealing of the damage. Adv. Mater. 2013; 25(7):1004-9.
[46] Banhart F, Kotakoski J, Krasheninnikov AV, Structural defects in graphene. ACS Nano 2010; 5(1):26-41.
[47] Zan R, Ramasse QM, Bangert U, Novoselov KS, Graphene reknits its holes. Nano Lett. 2012; 12(8):3936-40.
[48] Mathew S, Chan TK, Zhan D, Gopinadhan K, Barman AR, Breese MBH, et al., Mega-electron-volt proton irradiation on supported and suspended graphene: A raman spectroscopic layer dependent study. J. Appl. Phys. 2011; 110(8):084309-9.
[49] Hedström M, Cheng H-P, Molecular-dynamics simulations of nanoscale surface modification of si(111) via local excitation. Phys. Rev. B 2000; 62(4):2751-8.
[50] Urbassek HM, Kafemann H, Johnson RE, Atom ejection from a fast-ion track: A molecular-dynamics study. Phys. Rev. B 1994; 49(2):786-95.
[51] Toulemonde M, Assmann W, Trautmann C, Grüner F, Jetlike component in sputtering of lif induced by swift heavy ions. Phys. Rev. Lett. 2002; 88(5):057602.
[52] Bringa EM, Johnson RE, Jakas M, Molecular-dynamics simulations of electronic sputtering. Phys. Rev. B 1999; 60(22):15107-16.
[53] Jakas MM, Bringa EM, Johnson RE, Fluid dynamics calculation of sputtering from a cylindrical thermal spike. Phys. Rev. B 2002; 65(16):165425.
[54] Jakas MM, Bringa EM, Thermal-spike theory of sputtering: The influence of elastic waves in a one-dimensional cylindrical spike. Phys. Rev. B 2000; 62(2):824-30.
[55] Meftah A, Brisard F, Costantini JM, Hage-Ali M, Stoquert JP, Studer F, et al., Swift heavy ions in magnetic insulators: A damage-cross-section velocity effect. Phys. Rev. B 1993; 48(2):920-5.
[56] Ogawa H, Ohata T, Ishii K, Sakamoto N, Kaneko T, Dependence of secondary-electron emission on the emergent angle of frozen-charged h^{0} and h^{+} projectiles penetrating a thin carbon foil. Phys. Rev. A 2007; 76(2):024901.
[57] Richter V, Fizgeer B, Michaelson S, Hoffman A, Kalish R, Escape depth of secondary electrons induced by ion irradiation of submicron diamond membranes. J. Appl. Phys. 2004; 96(10):5824-9.
[58] Liu J, Neumann R, Trautmann C, Müller C, Tracks of swift heavy ions in graphite studied by

scanning tunneling microscopy. Phys. Rev. B 2001; 64(18):184115.